Japanese Journal of Radiology (2019) 37:651–659
https://doi.org/10.1007/s11604-019-00855-x

ORIGINAL ARTICLE

Liver imaging reporting and data system (LI-RADS) v2018: comparison between computed tomography and gadoxetic acid-enhanced magnetic resonance imaging

Sei Nakao[1] · Masahiro Tanabe[1] · Munemasa Okada[1] · Matakazu Furukawa[1] · Etsushi Iida[1] · Keisuke Miyoshi[1] · Naofumi Matsunaga[1] · Katsuyoshi Ito[1]

Received: 23 May 2019 / Accepted: 9 July 2019 / Published online: 18 July 2019

Abstract

Purpose To determine the consistency of major hepatocellular carcinoma (HCC) features between CT and MRI based on Liver Imaging Reporting and Data System (LI-RADS) v2018 and to investigate the additional value on gadoxetic acid-enhanced MRI.

Materials and methods Patients who underwent dynamic CT and gadoxetic acid-enhanced MRI within 1 month were investigated. Two radiologists evaluated the presence of major HCC features and categorized observations using LI-RADS v2018 algorithm. In addition, each observation was recorded as hyper-, iso-, or hypo-intensity on hepatobiliary-phase (HBP) images.

Results Sixty-one patients with 110 observations were identified. Among 88 observations classified as LR-3, 4 or 5, arterial phase hyper-enhancement and washout appearance showed higher frequencies on CT than on MRI (75.0% vs. 58.0%, $P < 0.001$, and 60.2% vs. 44.3%, $P = 0.014$, respectively). Of the 59 LR-3 observations categorized on MRI, 70.0% of observations with hypo-intensity on HBP images were HCCs, whereas 89.5% of observations with iso- or hyper-intensity on HBP images were non-HCCs ($P < 0.001$)

Conclusion The frequencies of arterial phase hyper-enhancement and washout appearances were higher on CT than on gadoxetic acid-enhanced MRI. For LR-3 observations, adding the hepatobiliary-phase hypo-intensity to major features improved the diagnostic performance of MRI in distinguishing HCCs from non-HCC lesions.

Keywords Liver imaging reporting and data system · Hepatocellular carcinoma · CT · Gadoxetic acid-enhanced MRI

Introduction

Hepatocellular carcinoma (HCC) is the most common primary liver cancer and the third leading cause of cancer death worldwide [1]. HCC can be noninvasively diagnosed in patients with chronic hepatitis or liver cirrhosis based on radiologic features without the requirement for histologic confirmation [2, 3]. To standardize the reporting and data collection of computed tomography (CT) and magnetic resonance imaging (MRI) for HCC, Liver Imaging Reporting and Data System (LI-RADS) was created by the American College of Radiology (ACR). The goals of LI-RADS are to reduce the variability in interpretation and improve communication with referring clinicians [4]. LI-RADS provides a diagnostic algorithm for the categorization of liver observations from LR-1 to LR-5 according to their likelihood of benignity or HCC [5]. For the characterization of liver lesions, it is necessary to evaluate the major HCC features of arterial phase hyper-enhancement, washout appearance, and capsule appearance. However, some studies reported substantial discordance between CT and MRI in LI-RADS categorization [6, 7], and showed that extracellular contrast agents (ECAs)-enhanced MRI had higher accuracy than CT in detecting HCC [8, 9].

Gadoxetic acid-enhanced MRI, which can provide both vascular phase imaging and hepatobiliary-phase (HBP) imaging, has been increasingly frequently used for the detection and characterization of HCC. Although LI-RADS v2013 applies only to CT and MRI performed with

✉ Masahiro Tanabe
itokatsu@yamaguchi-u.ac.jp

[1] Department of Radiology , Yamaguchi University Graduate School of Medicine , 1-1-1 Minami Kogushi, Ube 755-8505, Yamaguchi, Japan

ECAs, LI-RADS version v2014 allows the use of gadoxetic acid for MRI [4]. Recently, gadoxetic acid-enhanced MRI has been reported to show comparable sensitivity to CT for the diagnosis of HCCs using LI-RADS v2014 [10].

In this study, we examined the consistency of major HCC features for the LI-RADS categorization between CT and gadoxetic acid-enhanced MRI based on LI-RADS v2018, and investigated the additional value of HBP gadoxetic acid-enhanced MRI for the diagnosis of HCC.

Materials and methods

Patients

The institutional review board of our hospital approved this retrospective study and waived the requirement for informed consent. We retrospectively searched the institutional radiology information systems to identify patients with chronic hepatitis or liver cirrhosis between July 2009 and March 2014. We established the following inclusion criteria: (a) patients who underwent dynamic CT and MRI with gadoxetic acid within 1 month of each other, and (b) patients with liver observations which were seen on both CT and MRI. Demographic and clinical data were extracted from electronic medical records.

CT technique

CT examinations were performed on a 64-MDCT scanner (Somatom Definition or Sensation 64; Siemens Medical Solutions, Erlangen, Germany). The scanning parameters of CT were as follows: tube voltage of 120 kVp, 250–450 mA (automatically adjusted to the patient's body build), pitch of 0.9, 0.5 s/rotation, field of view (FOV) 35 cm, 512 × 512 matrix and section collimation of 0.6 mm. All images were reconstructed using a slice thickness and interval of 5.0 mm. The direction of all scans was cephalocaudal. After obtaining unenhanced images through the liver, triple-phase contrast-enhanced dynamic CT was performed after a bolus injection of almost 600 mg I/kg nonionic contrast medium. Contrast material was injected for 30 s using a power injector (injection rate: 3–5 ml/s, depending on the patient's weight). A bolus-tracking software program was used to trigger the hepatic arterial phase scans at 22 s after contrast enhancement of the upper abdominal aorta to an attenuation threshold of 100 HU. Portal venous phase and equilibrium-phase images were obtained 70 and 180 s after the start of injection of the contrast medium, respectively.

MRI technique

MRI was performed with a 1.5-T system (Magnetom Avanto; Siemens, Erlangen, Germany, or Signa CVi, GE Healthcare, Milwaukee, WI, USA) with a body phased-array coil. The MR sequences included axial breath-hold T1-weighted gradient echo in-phase and opposed-phase images and axial fat-suppressed breath-hold T2-weighted fast spin-echo images. Dynamic MRI was performed before and after the intravenous administration of 0.025 mmol/kg gadoxetic acid (Primovist; Bayer Schering AG, Berlin, Germany) flushed with 20 ml of saline using a power injector at a rate of 1 ml/s. For dynamic imaging, triple-phase images were obtained as follows: hepatic arterial phase (usually a 25-s fixed delay), portal venous phase (60-s delay), and transitional phase (180-s delay). The hepatobiliary phase (HBP) was obtained 20 min after contrast injection. Diffusion-weighted images were acquired after contrast injection using a respiratory-triggered single-shot echo-planar imaging sequence with *b* values of 0 and 1000 s/mm^2. The detailed sequence parameters are listed in Table 1.

Imaging data analyses

Two independent abdominal radiologists with 14 and 4 years of experience (MT, KM) reviewed CT and MR images. The readers were blinded to any clinical information except for the study population of patients with chronic hepatitis or liver cirrhosis. Two separate data sets (CT and MRI) were reviewed with a 4-week interval to minimize the recall bias. Any discrepancies in interpretation were resolved by consensus.

For each observation annotated on the CT and MRI findings by the radiologist (SN) who finally determined the study population but did not participate in the image review, each reviewer measured the diameter of the observation and evaluated the presence or absence of major HCC features (arterial phase hyper-enhancement, washout appearance, and capsule appearance). For gadoxetic acid-enhanced MRI, the washout appearance was determined only on the portal venous-phase images, avoiding the transitional phase or HBP images; in contrast, for CT, the washout appearance was determined on the portal venous-phase and/or equilibrium-phase images [4]. The radiologists also categorized the observations using the LI-RADS v2018 algorithm (LR-1: definitely benign, LR-2: probably benign, LR-3: indeterminate probability of malignancy, LR-4: probably HCC, LR-5: definitely HCC, and LR-M: probably or definitely malignant but not HCC specific). Ancillary imaging features were only used to assign LR-1

Table 1 Imaging parameters of gadoxetic acid-enhanced MRI

Protocol	Dual echo T1WI	T2WI	DWI[a]	Dynamic study	T1-CE
Magnetom Avanto, Siemens					
Sequence	GRE	Fast-SE	EPI	GRE	GRE
Slice	19	19	32	72	72
Section thickness (mm)	8	8	6	2.5	2.5
Repetition time (ms)	170	3740	5000	3.67	3.67
Echo time (ms)	2.3/4.8	83	76	1.4	1.4
Flip angle (°)	75	170	90	10	15
Fat saturation	No	No	No	Yes	Yes
Matrix	173×256	144×320	72×128	154×256	154×256
Field of view (mm)	360×270	360×270	360×270	360×270	360×270
Breathing	BH	BH	FB	BH	BH
Signa CVi, GE					
Sequence	GRE	fast-SE	EPI	GRE	GRE
Slice	19	17	20	48	72
Section thickness (mm)	8	8	8	8	5
Repetition time (ms)	150	2500	5000	5.9	5.9
Echo time (ms)	2.2/4.7	75	Minimum	1.3	1.3
Flip angle (°)	60	90	90	15	25
Fat saturation	No	No	No	Yes	Yes
Matrix	256×192	256×160	128×128	256×192	256×192
Field of view (mm)	350	350	450×338	350	350
Breathing	BH	BH	FB	BH	BH

CE contrast enhanced, *GRE* gradient echo, *SE* spin-echo, *EPI* echo-planar imaging, *BH* breath-hold, *FB* free-breathing

[a]*b* value of 0 and 1000 s/mm^2

or 2 categories, and the observations in LR-3, 4, or 5 categories were determined using only major HCC features. In the next step, the signal intensity on the hepatobiliary-phase images as the ancillary imaging feature were evaluated for the observations in LR-3, 4, or 5 categories. Each observation was recorded as hyper-, iso-, or hypo-intensity on the HBP images compared with background liver. As none of the prior CT or MRI findings were provided in the image analysis, threshold growth or visibility as discrete nodules at antecedent ultrasound was not used in the assignment of LI-RADS categories.

Statistical analyses

We evaluated the inter-observer agreements in assigning by kappa values as follows: poor agreement, 0.00–0.20; fair agreement, 0.21–0.40; moderate agreement, 0.41–0.60; good agreement, 0.61–0.80; and excellent agreement, 0.81–1.00. We used the McNemar test to assess statistically different sensitivities of LR-5 or LR-4 and 5 for the diagnosis of HCCs in each reviewer between CT and MRI. The frequencies of each major HCC feature were compared between CT and MRI using the McNemar test. Fisher's exact test was performed to compare the frequencies of HCC between the hypo-intensity and iso-/hypo-intensity groups on HBP images. *P* values of less than 0.05 were considered to indicate statistical significance.

All statistical analyses were performed with the EZR software program (version 1.38; Saitama Medical Center, Jichi Medical University, Saitama, Japan), which is a graphical user interface for R (The R Foundation for Statistical Computing, Vienna, Austria, version 3.5.3). More precisely, it is a modified version of R commander that incorporates statistical functions frequently used in biostatistics.

Results

Patients

This study included 110 observations in 61 patients (40 men and 21 women; mean age 67.6 years and age range 44–84 years). The clinical histories of the patients are shown in Table 2. CT was performed before MRI in 48 patients, with a mean (±standard deviation [SD]) time between studies of 16.7±8.1 days, and MRI was performed before

Table 2 The clinical histories

Characteristics	Patients ($n=61$)	
Age (years) *	67.6 ± 10.0 (range, 44–84)	
Male: Female	40:21	
Cause of liver disease		
Hepatitis C	24	39.3%
Hepatitis B	7	11.5%
Hepatitis B and hepatitis C	1	1.6%
Alcoholic cirrhosis	12	19.7%
Hepatitis B and alcohol	1	1.6%
Hepatitis C and alcohol	2	3.3%
Nonalcoholic steatohepatitis	4	6.6%
Cirrhosis of drags	1	1.6%
Cirrhosis of unknown cause	9	14.8%
Child–Pugh classification		
Class A	56	91.8%
Class B	5	8.2%
Class C	0	0.0%
Previous treatment for HCC		
Hepatic resection	4	6.6%
Hepatic resection and RFA	1	1.6%
TACE and RFA	2	3.3%
TACE	2	3.3%
RFA	1	1.6%
None	51	83.6%
No. of observations		
1	34	55.7%
2	16	26.2%
3	8	13.1%
4	1	1.6%
6	1	1.6%
10	1	1.6%

TACE transcatheter arterial embolization, *RFA* radiofrequency ablation

*Data are mean ± standard deviation

CT in 12 patients, with a mean time between studies of 10.5 ± 9.6 days. CT and MRI were performed on the same day in one patient.

Of the 110 observations, 59 were pathologically confirmed by surgery ($n=57$) or a percutaneous needle biopsy ($n=2$). These observations included 50 HCCs, 3 other malignancies (2 combined hepatocellular and cholangiocarcinoma and 1 lymphoma), and 6 benign lesions (1 dysplasia, 1 hepatic hemangioma, 1 schistosomiasis, and 3 pseudo-lesions). The remaining 51 observations were clinically diagnosed as HCC ($n=11$) or benign hepatic entities ($n=40$). The clinical diagnosis was based on a prior examinations and/or follow-up examinations. Therefore, a total of 61 HCCs were included in the present study.

Mean size of all observations ($n=110$) were 21.1 mm (range 4–135 mm). Regarding HCCs ($n=61$), mean size of the lesions was 25.8 mm (range 5–135 mm). Among these, 18 HCCs were less than 10 mm, 23 were 10–19 mm, and 20 were equal to or larger than 20 mm. Pathological diagnosis obtained in 50 of 61 HCCs included 11 well-differentiated, 36 moderately differentiated, 2 poorly differentiated, and 1 unclassified HCC.

LI-RADS scores between CT and MRI

The numbers of observations in each LI-RADS category on CT and MRI are shown in Table 3. LI-RADS categorization was conducted based on only major features in LR-3, 4, or 5 categories. The LI-RADS category differed between CT and MRI for 37 (33.6%) of 110 observations. Among these, LI-RADS score in CT was higher than that in MRI in 25 observations, while it was lower in CT compared with MRI in the remaining 12 observations. Regarding the frequency of LR-3 and 5 categorization, CT showed a higher frequency of LR-5 (31.8% [35/110] vs. 22.7% [25/110]) and a lower frequency of LR-3 (42.7% [47/110] vs. 53.6% [59/110]) than MRI (Table 3) (Fig. 1).

For the diagnosis of 61 HCCs, the PPV of LR-5 for the diagnosis of HCCs was 88.6% on CT and 92.0% on MRI. The PPV of LR-4 or 5 for the diagnosis of HCCs was 88.7% on CT and 91.2% on MRI. The sensitivities of LR-5 and LR-4 or 5 for the diagnosis of HCCs were not significantly different between CT and MRI (50.8% vs. 37.7%,

Table 3 Number of observations in each LI-RADS category on CT and MRI

LI-RADS category on CT	LI-RADS category on MRI					
	1	2	3	4	5	Total
1	9	1	1	–	–	11
2	3	1	3	–	1	8
3	2	1	39	3	2	47
4	–	–	5	3	1	9
5	–	–	11	3	21	35
Total	14	3	59	9	25	110

Dashes (–) indicate no observations in this category

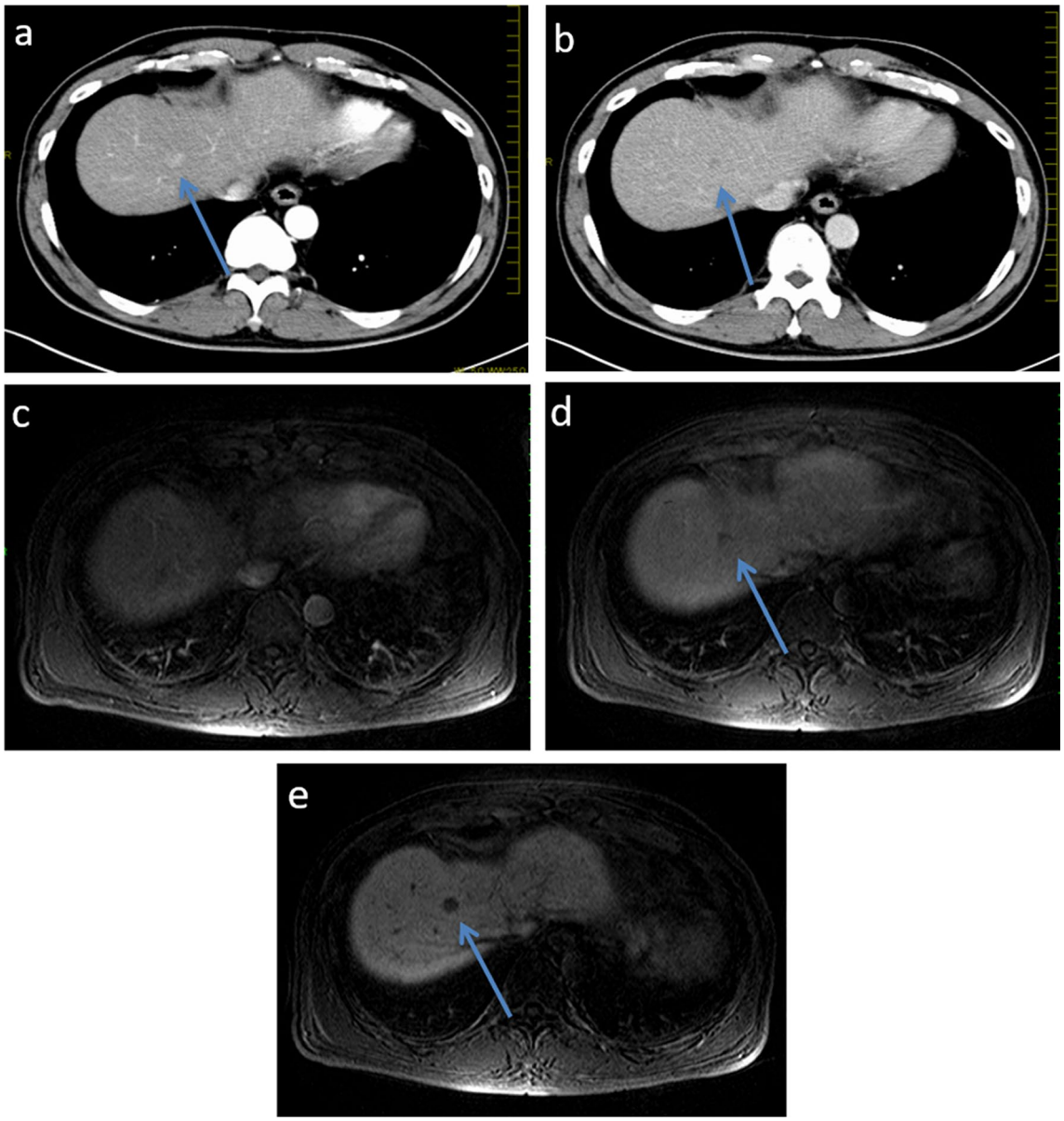

Fig. 1 Pathologically proven HCC with LR-4 categorization on CT and LR-3 on MRI. **a** Arterial-phase and **b**) equilibrium-phase CT showed 10 mm nodule with arterial enhancement and washout (arrows), consistent with LR-4 on CT. On the **c** arterial-phase and **d** portal venous-phase MRI, this nodule showed no arterial enhancement, but washout was observed (arrow), consistent with LR-3 on MRI. On the **e** hepatobiliary-phase MRI, this nodule was clearly demonstrated as hypo-intensity (arrow)

$P = 0.061$ and 64.0% vs. 50.8%, $P = 0.099$, on CT and MRI, respectively).

Major HCC features in LI-RADS and signal intensities on HBP images as an ancillary feature

The inter-observer agreements in assigning major HCC features on CT and MRI were good for arterial phase hyper-enhancement, fair-to-moderate for washout appearance, and moderate for capsule appearance. Comparisons of the frequencies of major imaging features of nodules classified LR-3 or higher between CT and MRI are shown in Table 4. Among the 88 observations classified as LR-3, 4, or 5 in both CT and MRI using the consensus method, the frequency of arterial phase hyper-enhancement and washout appearance was higher on CT than on MRI (75.0% [66/88] vs. 58.0% [51/88], $P < 0.001$; 60.2% [53/88] vs. 44.3% [39/88], $P = 0.014$), whereas the frequency of capsule appearance was not significantly different between CT and MRI (14.8% [13/88] vs. 10.2% [9/88], $P = 0.343$) (Table 4).

The frequencies of HCC between LR-3 observations with hypo-intensity and with iso-/hyper-intensity on HBP images

Table 4 Comparison of the frequencies of major imaging features of nodules classified LR-3 or higher between CT and MRI

Major features	CT	MRI	*P* value
Arterial phase hyper-enhancement	66 (75.0%)	51 (58.0%)	<0.001*
Washout appearance	53 (60.2%)	39 (44.3%)	0.014**
Capsule appearance	13 (14.8%)	9 (10.2%)	0.343

Data were compared using the McNemar test

*Significant value, $P<0.05$

Table 5 Comparison of the frequencies of HCC between LR-3 observations (CT: $n=47$, MRI; $n=59$) with hypo-intensity and iso-/hyper-intensity on HBP images

	HCC	Non-HCC	*P* value
CT ($n=47$)			
HBP hypo-intensity	20	8	<0.001*
HBP iso-/hyper-intensity	2	17	
MRI ($n=59$)			
HBP hypo-intensity	28	12	<0.001*
HBP iso-/hyper-intensity	2	17	

*Significant value, $P<0.05$

were compared (Table 5). Of the 47 LR-3 observations categorized on CT (HCC = 22, non-HCC = 25), 71.4% (20/28) of observations with hypo-intensity on HBP images were HCCs, whereas 89.5% (17/19) of observations with iso- or hyper-intensity on HBP images were non-HCCs ($P<0.001$) (Table 5). Similarly, of the 59 LR-3 observations categorized on MRI (HCC = 30, non-HCC = 29), 70.0% (28/40) of observations with hypo-intensity on HBP images were HCCs, whereas 89.5% (17/19) of observations with iso- or hyper-intensity on HBP images were non-HCCs ($P<0.001$) (Figs. 2, 3).

Discussion

LI-RADS is a comprehensive system for interpreting and reporting the liver observations in patients at high risk for HCC. LR-5 observations are considered to be HCC with nearly 100% certainty, and those may be treated as HCC without a liver biopsy. Our results showed that the PPV of LR-5 for the diagnoses of 61 HCCs was 100% on both CT and MRI, with non-significant difference in sensitivity of LR-5 for the diagnosis of HCCs between CT and MRI, indicating comparability between CT and MRI for the LR-5 category. Joo et al. also reported that the sensitivities of LR-5/5v were not significantly different between CT and gadoxetic acid-enhanced MRI [10].

Observations classified according to the LI-RADS v2014 categories are associated with different imaging outcomes. Tanabe et al. reported that the cumulative incidence of progression to a malignant category (LR-5 or LR-M) was higher for index LR-4 observations than for index LR-3 or LR-2 observations [11]. LI-RADS is intended to be used with both CT and MRI; however, recent studies have reported substantial discordance between CT and MRI in LI-RADS categorization [6, 7]. In this study, the LI-RADS category differed between CT and MRI for 37 (33.6%) of 110 observations, and it was higher in CT than in MRI in 25 of 37 observations. In addition, regarding the frequency of LR-5, CT showed a higher frequency of LR-5 than MRI. This fact may be due to the difference in visibility of major HCC features between CT and MRI. LI-RADS categories mainly concern the diameter of the observations and three major HCC features: arterial phase hyper-enhancement, washout appearance, and capsule appearance. In our study, arterial phase hyper-enhancement and a washout appearance were more frequent on CT than on MRI, whereas the frequency of capsule appearance was not significantly different between CT and MRI. This is important, as visualization of these two features is likely to induce higher categorization of the LI-RADS scores. Hope reported that arterial phase hyper-enhancement was seen more frequently on CT than MRI (90% vs. 63%, $P<0.001$) [12]. Joo et al. reported that a washout appearance was more frequently observed on CT than on MRI (87.0% vs. 69.0%, $P<0.001$) [10]. Due to the relatively small gadolinium dose and high frequency of arterial phase artifacts, gadoxetate acid-enhanced MRI may have lower sensitivity for arterial phase hyper-enhancement than ECA-enhanced MRI [13]. Regarding a washout appearance, hepatocyte uptake of gadoxetate acid may start as early as the end of the portal venous phase, and transitional phase hypo-intensity was not considered to indicate a washout appearance [14]. This may cause discrepancies in the frequency between CT and MRI.

Our study showed that, for LR-3 observations, adding the hepatobiliary-phase hypo-intensity to major HCC features improved the diagnostic performance of LI-RADS category for HCCs. Although LI-RADS v2014 incorporates hepatobiliary contrast agents into the diagnostic algorithm, some features unique to HBP imaging are included only as ancillary features [15]. Choi et al. reported that 94% of LR-3 observations identified on gadoxetic acid-enhanced MRI remained stable or decreased in category during imaging follow-up [16]. The most common cause of LR-3 observations is hyper-vascular pseudo-lesions, including arterioportal shunts [16]. This is supported by the fact that most of these observations showed arterial phase hyper-enhancement without a washout appearance or hepatobiliary-phase hypo-intensity. Chen et al. suggested that the use of an HBP image from gadoxetate acid-enhanced MRI as an additional major criterion improved the sensitivity of LI-RADS for distinguishing HCCs from

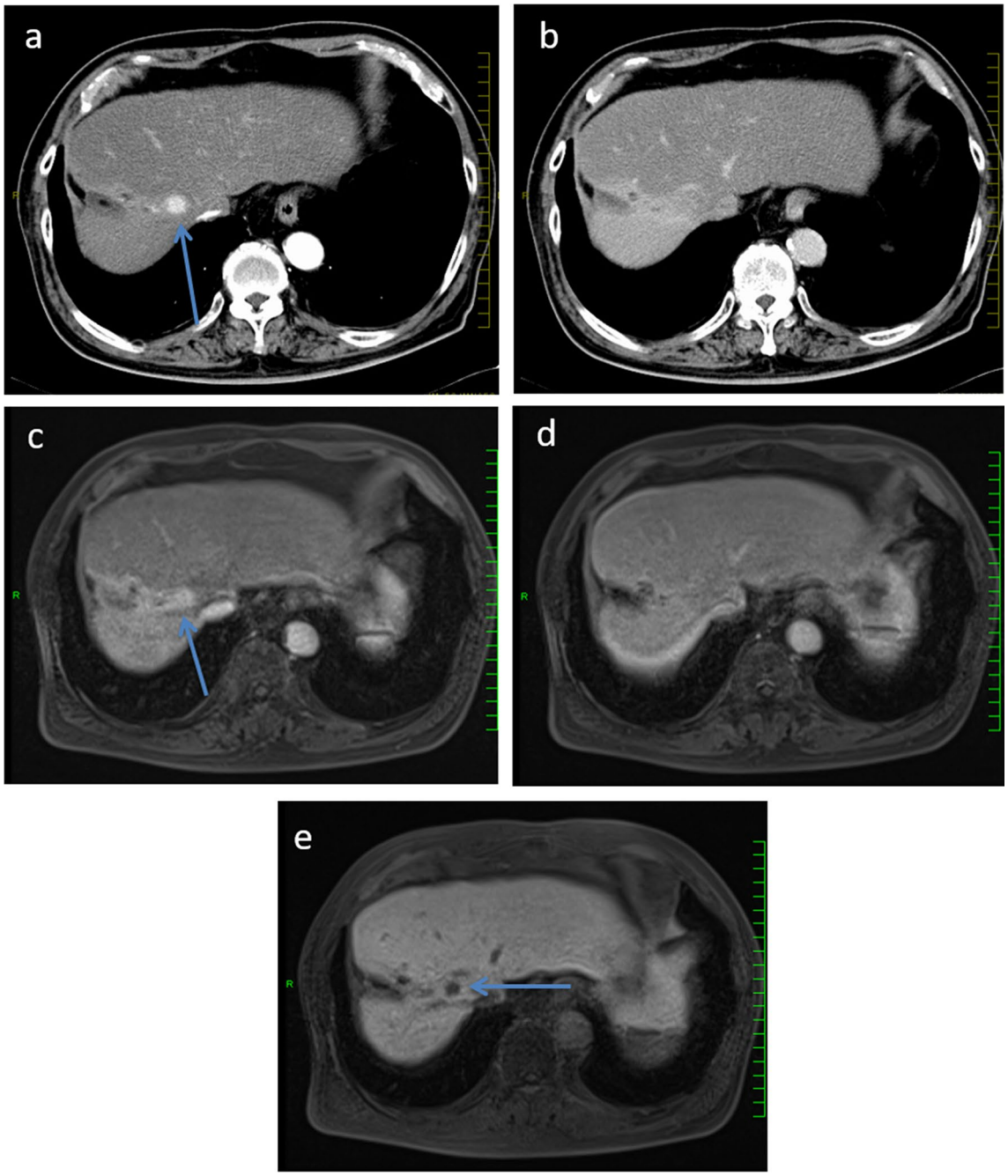

Fig. 2 Pathologically proven HCC categorized as LR-3 on both CT and MRI. **a** Arterial-phase and **b** equilibrium-phase CT. **c** Arterial-phase, **d** portal venous-phase, and **e** hepatobiliary-phase MR images. 13 mm nodule showed arterial enhancement on both CT and MRI (arrows in **a**, **c**), while washout and capsule were not observed, consistent with LR-3. On the hepatobiliary-phase MR image, this nodule was clearly demonstrated as hypo-intensity (arrows in **e**)

benign hepatic lesions while retaining high specificity [17]. The Liver Cancer Study Group of Japan also proposed a surveillance and diagnostic algorithm for HCC, reaffirming the extremely important role of gadoxetic acid-enhanced MRI [18].

Several limitations associated with the present study warrant mention. First, due to the retrospective nature of this study, patient selection bias may have been present. Our study consisted of patients who underwent both CT and gadoxetic acid-enhanced MRI within 1 month. However, this combination of CT and MR examinations had been usually limited to surgical candidates or patients with atypical imaging features. A prospective study with a large cohort is needed to confirm our results. Second,

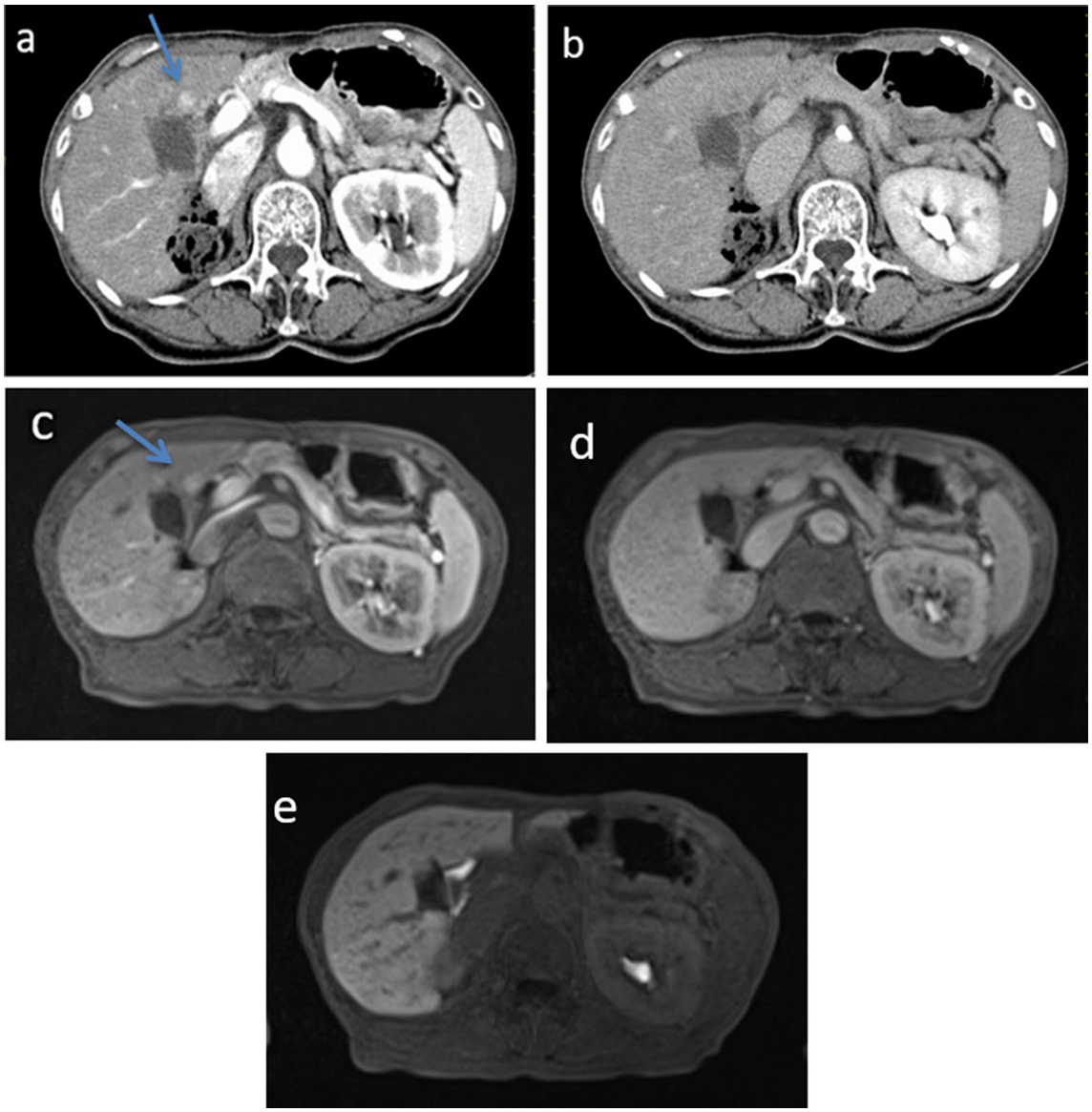

Fig. 3 Non-HCC categorized as LR-3 on both CT and MRI. **a** Arterial-phase and **b** equilibrium-phase CT. **c** Arterial-phase, **d** portal venous-phase, and **e** hepatobiliary-phase MR images. CT and MR images showed 17 mm nodule with arterial enhancement (arrows in **a**, **c**). However, washout and capsule were unclear, consistent with LR-3 observation. On the hepatobiliary-phase MR image, this nodule showed isointensity, compared with surrounding liver parenchyma

pathologic proof was lacked for some liver observations. At our institution, a liver biopsy is rarely performed to diagnose focal hepatic lesions; therefore, no pathology correlation could be assessed for any of the lesions. Third, the observations in the LR-3, 4, or 5 categories were determined using only major HCC features in this study. The precise effect of ancillary features is difficult to judge, as there are no strict guidelines regarding when ancillary features should be used to upgrade an observation [6]. Therefore, we focused on the major HCC features and the additional finding of hepatobiliary-phase hypo-intensity. Fourth, threshold growth was not used in the assignment of LI-RADS categories. Clinically, it is important to assess the threshold growth for an HCC diagnosis; however, none of the patients had undergone any prior examinations. This study focused on the imaging features obtained from a single examination. Finally, the timing of arterial phase for gadoxetic acid-enhanced MRI was fixed in this study, possibly affecting the difference of enhancement at arterial phase between CT and MRI [19]. In addition, gadoxetic acid -enhanced MRI at 3 T has been reported to yield better visualization of tumor recurrence after transcatheter arterial chemoembolization for HCC compared with dynamic CT [20].

In conclusion, the frequency of arterial phase hyperenhancement and washout appearances was higher on CT than on gadoxetic acid-enhanced MRI. For LR-3 observations, adding the hepatobiliary-phase hypo-intensity to major features improved the diagnostic performance of MRI in distinguishing HCCs from non-HCC lesions.

Compliance with ethical standards

Conflicts of interest The authors declare that they have no competing interests.

Ethical approval This study was approved by the Institutional Review Board of our institution.

References

1. Purysko AS, Remer EM, Coppa CP, Filho lHM, Thupili CR, Veniero JC. LI-RADS: a case-based review of the new categorization of liver findings in patients with end-stage liver disease. Radiographics. 2012;32(7):1977–95.
2. Bota S, Piscaglia F, Marinelli S, Pecorelli A, Terzi E, Bolondi L. Comparison of international guidelines for noninvasive diagnosis of hepatocellular carcinoma. Liver Cancer. 2012;1(3–4):190–200.
3. Bruix J, Sherman M. Management of hepatocellular carcinoma: an update. Hepatology (Baltimore, MD). 2011;53(3):1020–2.
4. American College of Radiology. Liver imaging reporting and data system. https://www.acr.org/Clinical-Resources/Reporting-and-Data-Systems/LI-RADS.
5. Mitchell DG, Bruix J, Sherman M, Sirlin CB. LI-RADS (Liver Imaging Reporting and Data System): summary, discussion, and consensus of the LI-RADS Management Working Group and future directions. Hepatology (Baltimore, MD). 2015;61(3):1056–65.
6. Corwin MT, Fananapazir G, Jin M, Lamba R, Bashir MR. Differences in liver imaging and reporting data system categorization between MRI and CT. AJR Am J Roentgenol. 2016;206(2):307–12.
7. Zhang YD, Zhu FP, Xu X, Wang Q, Wu CJ, Liu XS, et al. Liver imaging reporting and data system: substantial discordance between CT and MR for imaging classification of hepatic nodules. Acad Radiol. 2016;23(3):344–52.
8. Marin D, Di Martino M, Guerrisi A, De Filippis G, Rossi M, Ginanni Corradini S, et al. Hepatocellular carcinoma in patients with cirrhosis: qualitative comparison of gadobenate dimeglumine-enhanced MR imaging and multiphasic 64-section CT. Radiology. 2009;251(1):85–95.
9. Pitton MB, Kloeckner R, Herber S, Otto G, Kreitner KF, Dueber C. MRI versus 64-row MDCT for diagnosis of hepatocellular carcinoma. World J Gastroenterol WJG. 2009;15(48):6044–51.
10. Joo I, Lee JM, Lee DH, Ahn SJ, Lee ES, Han JK. Liver imaging reporting and data system v2014 categorization of hepatocellular carcinoma on gadoxetic acid-enhanced MRI: comparison with multiphasic multidetector computed tomography. J Magn Reson Imag JMRI. 2017;45(3):731–40.
11. Tanabe M, Kanki A, Wolfson T, Costa EA, Mamidipalli A, Ferreira MP, et al. Imaging outcomes of liver imaging reporting and data system version 2014 Category 2, 3, and 4 observations detected at CT and MR Imaging. Radiology. 2016;281(1):129–39.
12. Hope TA, Aslam R, Weinstein S, Yeh BM, Corvera CU, Monto A, et al. Change in liver imaging reporting and data system characterization of focal liver lesions using gadoxetate disodium magnetic resonance imaging compared with contrast-enhanced computed tomography. J Comput Assist Tomogr. 2017;41(3):376–81.
13. Cruite I, Tang A, Mamidipalli A, Shah A, Santillan C, Sirlin CB. Liver imaging reporting and data system: review of major imaging features. Semin Roentgenol. 2016;51(4):292–300.
14. Hope TA, Fowler KJ, Sirlin CB, Costa EA, Yee J, Yeh BM, et al. Hepatobiliary agents and their role in LI-RADS. Abdom Imaging. 2015;40(3):613–25.
15. An C, Rakhmonova G, Choi JY, Kim MJ. Liver imaging reporting and data system (LI-RADS) version 2014: understanding and application of the diagnostic algorithm. Clin Mol Hepatol. 2016;22(2):296–307.
16. Choi JY, Cho HC, Sun M, Kim HC, Sirlin CB. Indeterminate observations (liver imaging reporting and data system category 3) on MRI in the cirrhotic liver: fate and clinical implications. AJR Am J Roentgenol. 2013;201(5):993–1001.
17. Chen N, Motosugi U, Morisaka H, Ichikawa S, Sano K, Ichikawa T, et al. Added value of a gadoxetic acid-enhanced hepatocyte-phase image to the LI-RADS system for diagnosing hepatocellular carcinoma. Magn Reson Med Sci. 2016;15(1):49–59.
18. Kudo M, Matsui O, Izumi N, Iijima H, Kadoya M, Imai Y. Surveillance and diagnostic algorithm for hepatocellular carcinoma proposed by the Liver Cancer Study Group of Japan: 2014 update. Oncology. 2014;87(Suppl 1):7–21.
19. Nakamura S, Nakaura T, Kidoh M, Utsunomiya D, Doi Y, Harada K, et al. Timing of the hepatic arterial phase at Gd-EOB-DTPA-enhanced hepatic dynamic MRI: comparison of the test-injection and the fixed-time delay method. J Magn Reson Imaging. 2013;38(3):548–54.
20. Miyayama S, Yamashiro M, Nagai K, Tohyama J, Kawamura K, Yoshida M, et al. Evaluation of tumor recurrence after superselective conventional transcatheter arterial chemoembolization for hepatocellular carcinoma: Comparison of computed tomography and gadoxetate disodium-enhanced magnetic resonance imaging. Hepatol Res. 2016;46(9):890–8.